G. L. Fillmore
W. L. Buehner
D. L. West

Drop Charging and Deflection in an Electrostatic Ink Jet Printer

Abstract: This paper describes the drop charging and drop deflection processes in an electrostatic ink jet printer. Included in the discussion of drop charging are induction interaction effects and charge synchronization requirements, as well as design considerations for the charge electrode. In describing the parameters governing drop deflection, some drop placement errors are related to undesired interactions resulting from aerodynamic forces and electrostatic repulsion effects on the drops. A scheme for obtaining accurate drop placement in the presence of these interaction effects is described.

Introduction

In an electrostatic ink jet printer [1], lines of characters are produced by deflecting charged drops vertically while the ink jet printhead moves horizontally relative to the paper. Here, we are concerned only with drop charging and drop deflection, the processes required to form vertical scans. In the charging process stored character data are converted to a temporal sequence of charge electrode voltages; for each drop to be charged, a voltage induces a charge on the stream at the point of drop breakoff. The charged drop is then deflected as it passes through an orthogonal electric field so that it strikes the paper at a height determined primarily by its charge and, to a lesser extent, by interactions with surrounding drops in flight. When a particular spot in the character matrix is to be left white, the uncharged drops are directed into a gutter and returned to the ink supply for recirculation.

Charging and deflection of ink drops for printing applications have been treated comprehensively by Sweet [2] and more recently reviewed by Kamphoefner [3]. The work reported in this paper was aimed at developing a printer capable of producing ink jet printing of a quality equivalent to that attained with a SELECTRIC® typewriter. The constraints imposed by this requirement demanded consideration of many second-order effects to develop suitable drop charging and drop deflection methods.

The drop charging process and related issues are described in the first part of this paper. The second part deals with drop deflection and the measurement and correction of drop placement errors.

Drop charging process

Before each drop of ink breaks off from the cylindrical jet, it can be either selectively charged and used to form part of a character, or it can be allowed to proceed to a gutter for ultimate recirculation. The charge is applied to a drop as the drop passes through an electrode centered

Figure 1 Drop charging with parallel plate electrodes.

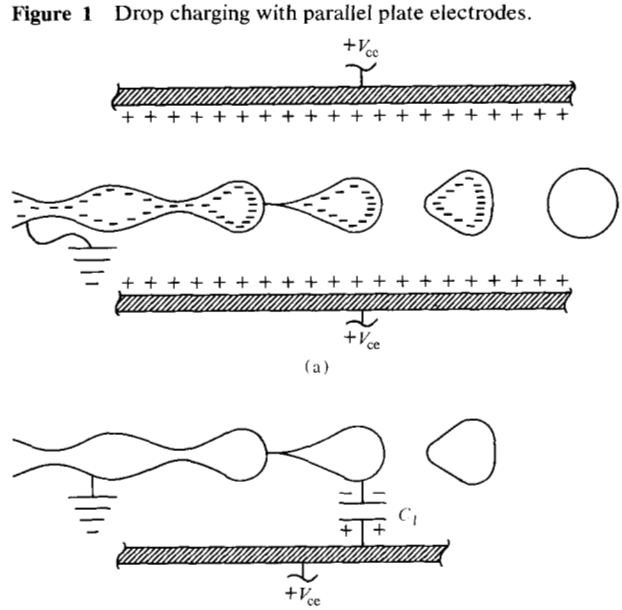

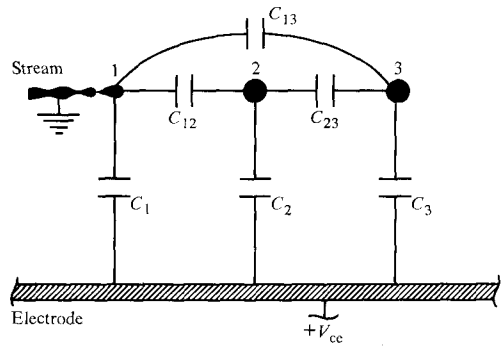

Figure 2 Equivalent charging circuit for two previously formed uncharged drops.

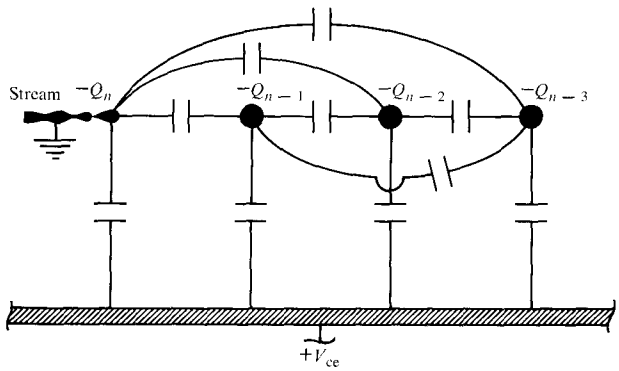

Figure 3 Equivalent circuit for three previously charged drops.

about the jet axis at the nominal stream breakup point. The amount of charge is determined by the relative level of a voltage pulse applied to the charge electrode, and that level is approximately proportional to the desired drop position relative to the character baseline on the printing surface.

An ink stream with two parallel-plate electrodes located at the point of breakup is shown in Fig. 1(a), with the equivalent electrical circuit as in Fig. 1(b). The conductive ink stream is grounded. The forming drop is one plate of capacitor C_1 between the stream and the electrode. When a voltage of the polarity shown is applied to the electrode, a negative charge is induced on the drop and is retained after breakoff until the drop impinges on the paper.

• *Inductive charge interactions*

The charge on a forming drop is influenced not only by the charge electrode potential but also by the charges on previously formed drops. In the presence of two previously formed but uncharged drops, the equivalent charging circuit is modified as shown in Fig. 2. With the additional charging paths shown, we can lump the various capacitive paths to the forming drop into one equivalent capacitor, C_e. Then the desired drop charge Q_n can be described by

$$Q_n = -C_e V_{ce}. \tag{1}$$

To illustrate the interactions among previously charged drops and the forming drop, the case of three previously charged drops is depicted in Fig. 3, which shows the drop-to-drop capacitive interactions from the three preceding drops that affect the net charge induced on the forming drop. In this case we must add three terms to Eq. (1) to describe drop charging:

$$Q'_n = -C_e V_{ce} + \Delta Q_{n-1} + \Delta Q_{n-2} + \Delta Q_{n-3}. \tag{2}$$

Here, Q'_n, which is less than the desired charge Q_n, must be increased by the amount $\Delta Q_{n-1} + \Delta Q_{n-2} + \Delta Q_{n-3}$ (the positive charges induced on the forming drop by each of the preceding drops).

For convenience, we define the following drop interaction constants:

$$\alpha = -\Delta Q_{n-1}/Q_{n-1}, \tag{3}$$

$$\beta = -\Delta Q_{n-2}/Q_{n-2}, \tag{4}$$

$$\gamma = -\Delta Q_{n-3}/Q_{n-3}. \tag{5}$$

Substituting Eqs. (3), (4), and (5) into (2), we obtain

$$Q'_n = -C_e V_{ce} - \alpha Q_{n-1} - \beta Q_{n-2} - \gamma Q_{n-3}. \tag{6}$$

We now use Eq. (6) to develop the charge equations (including induction interaction effects) for four consecutive charged drops. Assume several uncharged drops prior to the formation of drop $n-3$. Then,

$$Q_{n-3} = -C_e V_{n-3}, \tag{7}$$

$$Q_{n-2} = -C_e V_{n-2} + C_e \alpha V_{n-3}, \tag{8}$$

$$Q_{n-1} = -C_e V_{n-1} + C_e[\alpha V_{n-2} + (\beta - \alpha^2) V_{n-3}], \tag{9}$$

$$Q_n = -C_e V_n + C_e[\alpha V_{n-1} + (\beta - \alpha^2) V_{n-2} - (\alpha^3 - 2\alpha\beta + \gamma) V_{n-3}], \tag{10}$$

where V_n, V_{n-1}, V_{n-2}, and V_{n-3} represent the charge electrode voltages for drops n, $n-1$, $n-2$, and $n-3$, respectively.

Measured interaction constants in our ink jet printer were $\alpha = 0.15$, $\beta = 0.045$, and $\gamma = 0.015$. If we take a simple case in which $V_n = V_{n-1} = V_{n-2} = V_{n-3}$, we find that Q_n is reduced 22 percent below its expected value when drops n − 1, $n-2$, and $n-3$ are uncharged. Drop charge changes of this magnitude cause unacceptably large drop placement errors. This decrease in charge is compensated by increasing the charge electrode voltage.

Drop placement correction techniques that involve adjusting the charge electrode voltage for these effects are also used to compensate for aerodynamic interaction and for mutual repulsion among drops in flight. A method for compensating all the drop interaction effects is described later.

• *Charge electrode design considerations*

Two charge electrode geometries were considered—a cylinder and parallel plates. A cylindrical electrode would have better charging efficiency, but the stream would be much more difficult to align in a two-dimensional configuration. Moreover, viewing the stream at breakup within the electrode would be difficult. Parallel plates facilitate stream alignment and, if the plates are oriented in the vertical direction, a stroboscopic light source can be placed under the electrode structure to permit viewing of the stream from above at breakup. Also, a vertical parallel-plate structure is less susceptible to contamination by ink during stream startup/shutdown cycles. Thus we chose the vertical parallel plate design.

The charge electrode should appear infinitely long within the range of expected excursions of the stream breakup point. Otherwise, variations in charging efficiency and induction interaction effects may become unacceptably large. The spacing of the parallel plates should be small in order to obtain high charging efficiency. On the other hand, it is desirable to have a large drop-to-electrode distance to allow for stream misalignment and the oversize drops that are sometimes formed at start-up. Plate separation s_{ce} in our charge electrode is 0.64 mm (25 mils) and plate length l_{ce} is 2.67 mm (105 mils).

A mathematical model of the parallel plate charge electrode was derived using the method of images [4]. The relationships among charging efficiency, induced charge, stream misalignment, plate spacing, and wavelength-to-jet diameter (λ/d_j) ratio were calculated with the model. The image model, although not a rigorous solution to the drop charging problem, proved useful in indicating general trends. Assumptions in the model include a spherical drop at breakup and an approximation of the ink drops as point charges. The model did not account for the grounded stream between the plates.

Figure 4 shows the first-order induced charge (percentage of charge from the previously charged drop to the drop being formed) as a function of λ/d_j for three parallel-plate electrode spacings. (A glossary is provided in Appendix 1.) The circled data point represents an experimental measurement on the printer. Variations in induced charge and charging efficiency as functions of stream misalignment within the charge electrode are shown in Figs. 5 and 6, respectively, for various parallel-plate electrode spacings.

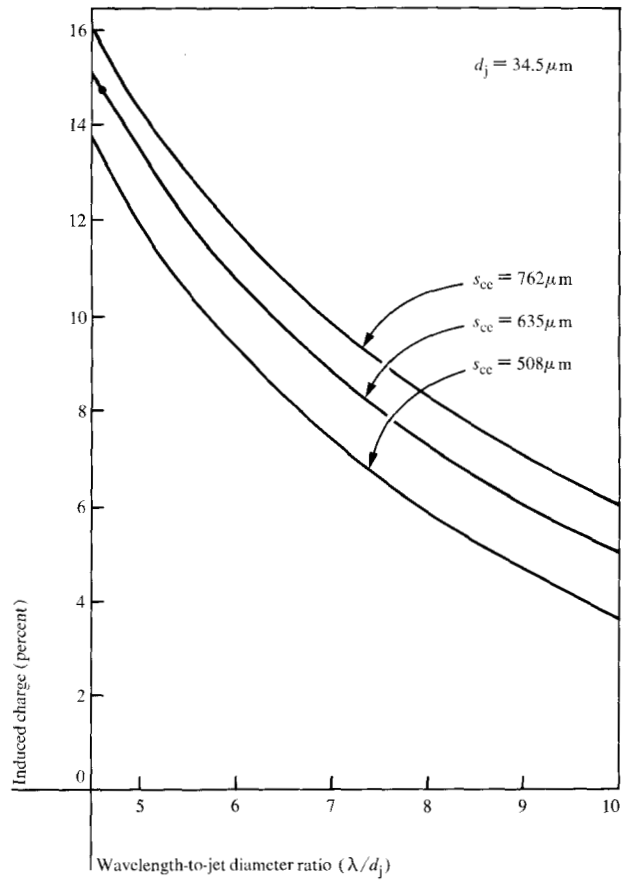

Figure 4 Induced charge vs wavelength-to-jet diameter ratio.

Figure 5 Induced charge vs stream misalignment.

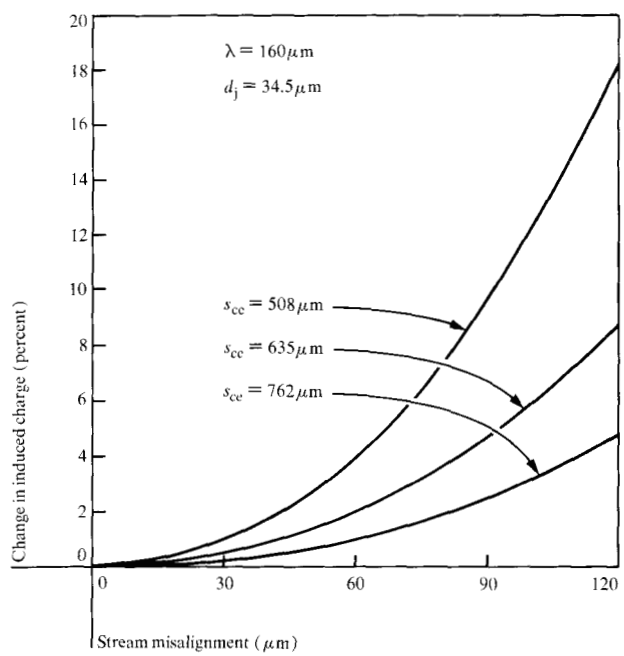

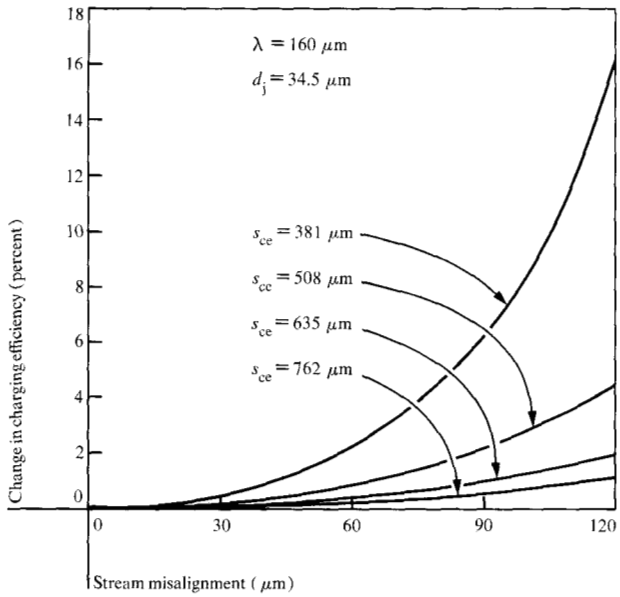

Figure 6 Charging efficiency vs stream misalignment.

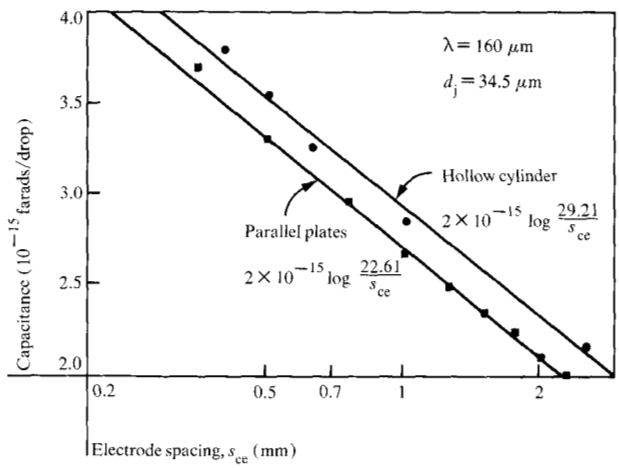

Figure 7 Charging efficiency vs electrode spacing.

The equivalent charging capacitance discussed earlier is useful as a measure of charge electrode efficiency and may be determined experimentally by placing a constant voltage on the electrode and measuring the current carried by the stream. Figure 7 shows charging efficiency versus electrode spacing for streams centered within a parallel-plate and a hollow cylinder charge electrode. Both sets of data are closely approximated (within ±3 percent) by an equation of the form

$$C_e = K \log_{10} \frac{s_0}{s_{ce}}, \tag{11}$$

where s_{ce} is the electrode spacing or diameter. Here s_0, the empirically derived constant, is 29.21 mm (1150 mils) for the cylindrical case and 22.61 mm (890 mils) for the parallel-plate configuration, and K is 2×10^{-15} F.

• *Maximum charging limits*

Two fundamental processes limit the amount of charge that can be placed on a drop. If the electrostatic repulsion forces are strong enough to overcome the surface tension that holds the drop together, the drop disintegrates. This limit [5] is given by

$$Q_{max} = (64\pi^2 \epsilon_0 r_d^3 \sigma)^{\frac{1}{2}} \text{ coulombs}, \tag{12}$$

where ϵ_0 is the permittivity of free space, r_d is the drop radius, and σ is the ink surface tension.

The second charging limitation is caused by the mutual electrostatic repulsion among the charged drops. This interaction among drops in flight can become so large that a small radial disturbance on a drop at breakup causes the stream to disperse at some distance down the jet axis. For a stream of drops that are all charged to the same level, we have found that the following empirical relation is valid over a wide range of the operating parameters for our printer:

$$\frac{Q_{max} z_i}{v_j d_j \lambda^2} = 1.05 \times 10^{-3} \frac{\text{coulomb-second}}{\text{metre}^3}, \tag{13}$$

where z_i is the distance from breakup to the point at which the average displacement from the jet axis is one drop radius, and v_j is the jet velocity. A derivation of the form of this equation is given in Appendix 2.

Although either of the above processes may limit maximum charge, for most ink jet systems the limit given by Eq. (13) is encountered first.

• *Charge synchronization*

In our ink jet printer, a discrete voltage level must be present on the charge electrode for each drop formed. This level must be applied for a sufficient interval prior to drop breakoff for the charge to build up to its desired value; this level must also be maintained until the drop breaks off. Some time is then required to change the voltage level to the value required for the next drop, but the voltage must not change until after the original drop has broken off from the stream.

Although the timing of the charge voltage pulse can be controlled electronically with sufficient accuracy, stream breakup time varies with ink temperature and pressure and with drop generator drive voltage, all of which have long-term variations. The correct timing relationship can be maintained by periodically adjusting the phase of the voltage pulse to coincide with the instant of stream breakup. Stream breakup time can be resolved within a fraction of one drop time period by applying a series of

variable-phase test charging signals to the charge electrode and directly or indirectly sensing drop charge to determine which signal actually charged the stream.

An obvious approach to obtaining an indication of drop charging for synchronization is to collect the charged drops in a metal container connected to ground through a picoammeter. The picoammeter would indicate the net current of the charges carried by the drops. Another sensing method would allow deflected drops to impact a force transducer (a piezoelectric element). Because only charged drops are deflected, drop impact on the transducer would indicate synchronization. In the method used in our printer, the drop charge is sensed by capacitive induction to a special sensing electrode. This electrode is also used for sensing and control of the deflection height [6].

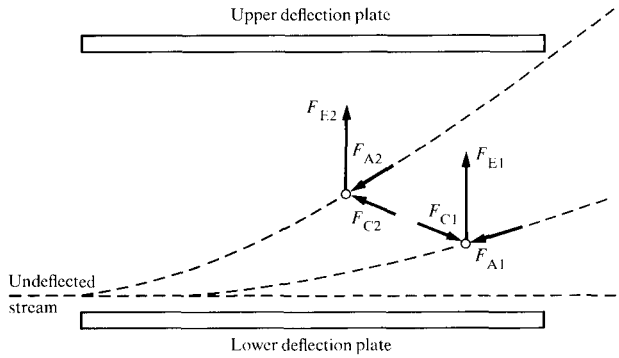

Figure 8 Electrostatic repulsion and aerodynamic interaction effects.

Vertical drop deflection

• *Deflection sensitivity*

After leaving the charge electrode, charged drops are deflected by an electric field to a height at the paper plane that is approximately proportional to their charge level. The deflection of an ink jet system can be approximated by the equation describing the defiection of a point charge in a uniform electric field:

$$x_d = \left(\frac{Q_d E}{m_d v_d^2}\right) l_{dp}\left(z_p - \frac{l_{dp}}{2}\right), \tag{14}$$

where x_d is drop deflection height, Q_d is drop charge, m_d is drop mass, E is electric field, l_{dp} is deflection plate length, and z_p is the distance from the deflection plate entry to the paper plane.

Two primary requirements for drop deflection are 1) that deflection be sufficiently large to meet character height needs, and 2) that deflection variations be accurately controlled to minimize character height changes. When considering variations in deflection, the geometric factors (z_p and l_{dp}) can be assumed to be unchanging. Drop frequency and deflection voltage, which affect the mass and electric field, respectively, are not difficult to control. Variation in charge synchronization (the primary cause of charge variation) has just been discussed. The details of adjusting velocity to maintain the correct deflection range are presented in [6]. We note here only that the deflection control system, which is needed primarily for compensating velocity variations, actually corrects the deflection, regardless of the parameter that caused the deflection height variation.

Drop deflection is increased either by increasing Q_d, E, l_{dp}, and z_p or by decreasing m_d and v_d. The limitations on increasing Q_d were discussed earlier. Electric field strength, E, can be increased only to the value at which air breakdown occurs under worst-case conditions of temperature and pressure [7]. Plate length, l_{dp}, cannot exceed z_p. It must, in fact, be somewhat smaller to accommodate the gutter and fog collection hardware [1]. The value of m_d is constrained by the required dot size to be printed. The lower limit on v_j (closely approximated by v_d) is determined primarily by its effect on wavelength (drop spacing), λ, and frequency, f, through the relation

$$v_j = f\lambda. \tag{15}$$

A decrease in f lowers the print rate. A decrease in λ affects drop generator performance, which is sensitive to the ratio λ/d_j. A decrease in λ or an increase in z_p also adversely affects drop merging, which is discussed later.

• *Drop placement errors*

To produce typewriter print quality with an ink jet printer, a relative dot placement tolerance of ±0.033 mm (±1.3 mils) is required, and overall character height must be controlled to within about 2 percent. The largest sources of drop placement errors are deflection errors, and among the latter, by far the largest deviation from the deflection predicted by Eq. (14) is caused by aerodynamic and electrostatic forces.

A free-body force diagram of two adjacent drops in flight is shown in Fig. 8. Vertical upward forces F_{E1} and F_{E2} are generated by the deflection field; aerodynamic drag provides retarding forces F_{A1} and F_{A2} along the trajectories; and forces F_{C1} and F_{C2} acting along the drop-to-drop axis are due to electrostatic repulsion. Vertical downward forces due to gravity are insignificant and thus are not shown.

The decreased velocity of a stream of drops due to air drag eventually causes the drops to merge unless acted upon by other forces. Aerodynamic effects on a stream of drops are further complicated by the fact that only the first drop in the stream is traveling through still air. The

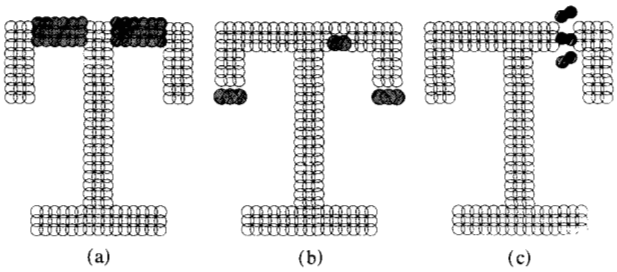

Figure 9 Drop placement error examples: (a) misplacement, (b) merging, (c) scattering.

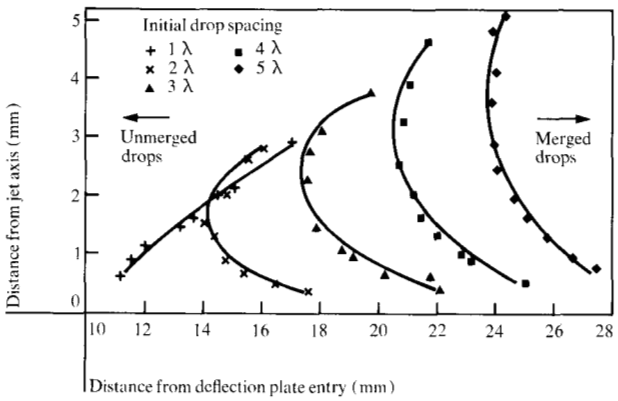

Figure 10 Merge curves.

remaining drops experience air turbulence and reduced drag due to the passage of their predecessors.

A delicate balance exists between the aerodynamic forces that tend to merge the drops and the electrostatic repulsion forces that tend to scatter them. Assume that two adjacent and charged drops in a stream of uncharged drops are entering the deflection field. While still in the mainstream, the two drops experience identical aerodynamic conditions, both flying in the wake of all preceding drops. As these two charged drops are deflected out of the mainstream, the leading drop ultimately travels through almost still air and is exposed to maximum drag. The trailing drop experiences a drag that is greater than that in the mainstream but less than the drag acting on the leading drop, since it moves in the wake of the latter. As the differential drag causes the distance between the drops to decrease, the repulsive electrostatic forces increase and give rise to drop scattering.

These effects are illustrated in the simulated ideal characters shown in Fig. 9. Note the difference in the height of the crossbar of the character T relative to the main stem height in Fig. 9(a). The long white space between the base and crossbar of the T represents a period during which several drops were undeflected. Thus, aerodynamic drag caused the first drops of the short vertical segment in the crossbar to be slowed and therefore deflected upward more than drops at the top of the adjacent long vertical segment in the stem of the T. Drag may also cause a leading drop to be slowed sufficiently so that the drop following merges with it, as shown in Fig. 9(b). This can be either a consistent effect, as at the bottom of the serifs, or an intermittent effect, as in the crossbar. The drop placement problem illustrated in the crossbar of the T, Fig. 9(c), is an example of a possible merge-scatter interaction. The leading drop of the short vertical segment is slowed, and the second drop comes very close to the leading drop. When this occurs at large deflection, the electrostatic repulsion force may overcome the aerodynamic forces tending to merge the two drops, resulting in drop scattering. This scattering effect may also be intermittent because of the highly unstable balance of these forces.

- *Experimental methods for characterizing drop interactions*

During the process of defining a combination of ink jet parameters to meet specific printer performance requirements, it became necessary to understand in detail the various drop interaction effects, so that a suitable scheme for accurately placing drops could be developed. The trajectory of a single drop can be described analytically even in the presence of the aerodynamic and electrostatic forces, but for a group of drops with their associated wakes, the problem becomes extremely complex. In the absence of any analytical means for studying drop interaction effects, some heuristic tools were developed. Two of the most useful characterization methods are merge curves and minimum separation curves [8].

Merge curves were generated by the following experiment: Two drops in a stream of otherwise uncharged drops are charged such that both follow the same deflection trajectory. Since the second drop is traveling in the wake of the first, it experiences a smaller drag force. If this difference in drag is not sufficiently counteracted by electrostatic repulsion forces, the second drop eventually overtakes the first and they merge into a single oversized drop. A merge curve is defined as the set of coordinates at which merging occurs. A different merge curve can be obtained for each initial spacing of the two drops. (Some merge curves are shown in Fig. 10.)

Because the wake of the undeflected stream reduces the differential drag of the two drops, the merge curves bend sharply to the right near the abscissa. As drop charge is increased, electrostatic repulsion between the drops becomes increasingly significant, causing the bending to the right at large deflections. The curves end abruptly at very large deflections, when the electrostatic forces become strong enough to prevent merging. One

additional characteristic worth noting is the crossing of the curves for different initial spacings. The aerodynamic forces fall off less rapidly than the $1/r^2$ electrostatic force. It is therefore possible for two drops separated by several wavelengths to build up a relative momentum that cannot be overcome by the electrostatic force, whereas this same electrostatic force is more than sufficient to prevent merging when the drops are initially separated by some smaller distance. One therefore cannot claim that increasing the drop spacing retards merging. In fact, increasing the separation between deflected drops may enhance merging. This phenomenon is an essential feature of the drop placement scheme (described later) used in our printer.

The utility of the merge curves is not limited to providing an understanding of the important parameters associated with drop merging. The area beyond the curves (Fig. 10) represents a region in which multiple drops may not be directed to a given deflection position without merging. For example, the minimum abscissa coordinate of the 1λ curve gives an approximate maximum distance between the deflection field entrance and the print plane if every drop is to be used. For a printer design these merge data have to be supplemented by two additional considerations: First, the curves are based on two-drop experiments; for many drops the picture becomes more complicated and smaller merge-free distances may have to be used. Second, since most ink jet printers do not send two drops to the same position at the paper plane, the second drop is not following directly in the wake of the first and the merging is, therefore, delayed.

Once a position for the paper plane has been chosen, it is useful to determine how closely consecutive drops can be placed on the paper. In Fig. 11(a) two drops are deflected to widely separated positions at the paper plane. The drop charges are then modified so that the impact points of the drops approach one another, as shown in Fig. 11(b). If the paper plane is located to the right of the merge boundary, and the drop charges are further changed to reduce the distance between the drop impact points, a condition is reached in which a single merged drop arrives at the paper plane, as illustrated in Fig. 11(c). The difference in impact points just before the merge occurs is called the minimum separation distance. Impact points separated by less than this distance cannot be addressed by individual drops. Thus, the minimum separation data set a maximum limit on the dot matrix resolution of an ink jet printer for a given operating point.

Figure 12 shows a typical set of minimum separation curves. The minimum separation distance is plotted as a function of height above the undeflected stream, and the initial spacing of the two drops is used as a parameter for the curves. These curves represent data taken for an ascending scan, i.e., the trailing drop was directed above the leading drop. A descending scan produces similar, though not identical, curves. Note that under certain

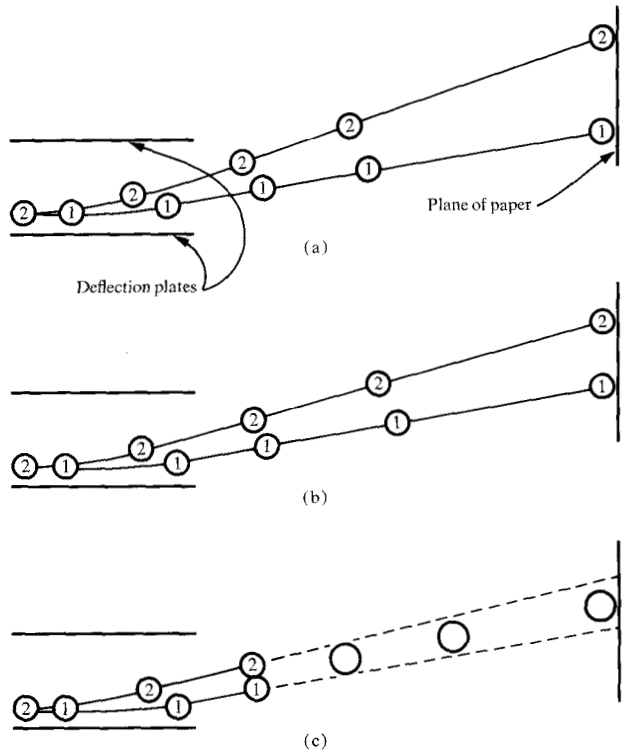

Figure 11 Drop merging and scattering.

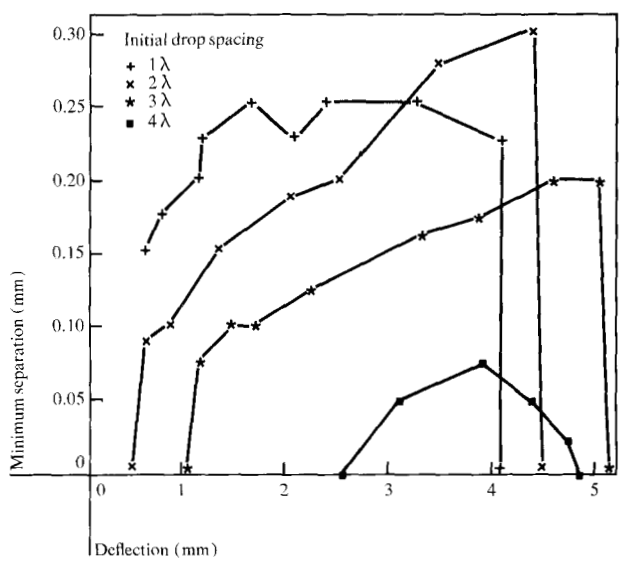

Figure 12 Minimum separation curves.

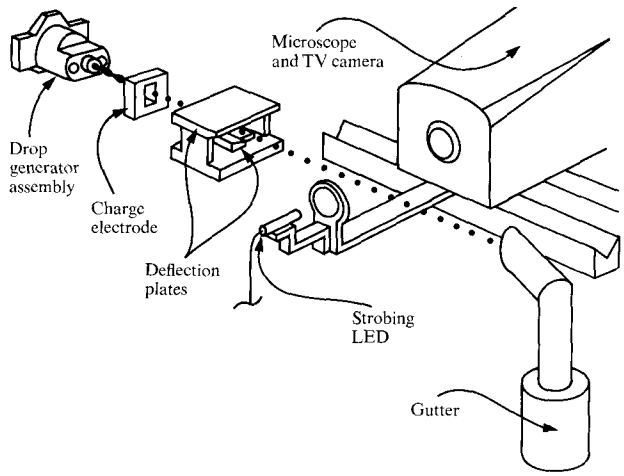

Figure 13 Setup for viewing ink jet stream.

conditions, drops that are separated initially by 1λ can actually be placed closer together than those starting with a 2λ spacing.

When the paper plane is located to the left of all the merge boundaries, the minimum separation is obviously zero. However, locating the paper plane at such a position unduly limits the deflection that can be obtained.

The paper plane position and character matrix resolution cannot be rigorously determined from these simple two-drop experiments. Significant interactions can occur between drops separated by ten wavelengths or more. It was therefore necessary that tentative conclusions drawn from these experiments be thoroughly re-examined using more complex drop patterns with each of the drop placement schemes considered later. The final qualification of operating parameters, including paper plane position and matrix resolution, was made only after satisfactory printing of characters in all fonts had been demonstrated.

Figure 13 shows the experimental equipment used for the drop position measurement on which the above trajectory characterization methods have been based. A microscope and closed-circuit television camera, together with a light-emitting diode (LED) and its associated focusing lens, were mounted on a platform, horizontally movable by micrometer control to permit viewing of the ink jet stream at any point between the nozzle and paper plane. The stream was illuminated by the LED and strobed at the drop generation frequency. A digital micrometer also provided vertical control of the viewing apparatus to measure drop deflection.

To control drop charging, an electronic robot was designed to generate the charging voltage for each of 256 sequential drops to be varied independently. Any drop in the 256-drop sequence could be selected by setting switches, and the charging voltage could be continuously varied by a switch-controlled up-down counter. This feature was particularly useful in varying individual drop charges to study merging and scattering. The signal used to pulse the LED was generated by delaying a signal that was synchronized with the first drop of the sequence. Because this delay was variable, a particular drop could be observed at any point in its flight path by adjusting the horizontal position of the viewing apparatus and controlling the timing of the LED pulse.

• *Drop placement schemes*

Various drop placement techniques were investigated to avoid the merge-scatter problems. The most obvious method of placing the drops at the paper plane is a sequential placement scheme in which print positions of drops used to form a vertical scan, listed in the order of their generation, form a monotonic sequence. The sequence can be either increasing (ascending scan) or decreasing (descending scan). Figure 14 is an example of a sequential drop placement scheme with ascending scans. The numbers on the drops indicate their generation order.

It is possible that the desired operating characteristics of an ink jet printer (deflection height, resolution, etc.) cannot be achieved with a sequential drop placement scheme, regardless of the choice of printhead parameters, because of the tendency of the first drops in a scan to merge. This merging can be prevented by placing drops on the paper in a nonsequential manner. Drops that are generated close together in time are widely spaced on the paper, and drops that are close on the paper are widely separated in time. Figure 15 illustrates two methods of nonsequential drop placement. An undesirable characteristic of this scheme, when used for printing single scans, Fig. 15(a), is the horizontal drop displacement caused by the motion of the ink jet printhead from left to right. An additional disadvantage of a nonsequential scheme is that one must consider a greater number of surrounding drops when making corrections for drop placement errors.

A third scheme consists of placing drops nonsequentially to form vertical segments of a character with certain drops from several successive scans. In this interlace scheme the separation of drops in a scan is chosen so as to avoid the merge-scatter problem. In Fig. 15(b), each vertical segment is formed from drops placed in three different scans, resulting in a "three-level interlace." The tilt of these segments, which is three times that of a sequential scan, can be corrected by tilting the deflection plates. By means of the interlace scheme, drops can be accurately placed without loss of through-

put. However, this method has two disadvantages: In addition to the extended range of correction required for the nonsequential schemes described earlier, it is necessary to have precise velocity control of the ink jet printhead, since a vertical segment involves several scans and a deflection plate tilt proportional to printhead velocity.

The fourth method of avoiding the merge-scatter problem is to increase the spatial separation between printed drops by inserting guard drops (uncharged drops) between the deflected drops [9]. The tendency of printed drops to merge is not uniform throughout a segment. The leading drops of a segment experience the most severe aerodynamic forces and therefore exhibit the strongest tendency to merge. Because more guard drops are required at the beginning of a segment to prevent merging, a scheme for inserting guard drops uniformly throughout a segment is inefficient.

A special "1032" guard drop scheme (named for the particular pattern of guard drops within the leading part of a segment) was empirically developed for our ink jet printer. This scheme, illustrated schematically in Fig. 16, attempts to minimize the print quality deterioration caused by merging, while minimizing the loss in throughput resulting from the use of guard drops. In an ascending scan each printed drop is placed one position higher in the character matrix than its predecessor. The only exceptions to this are the first two drops, which are allowed to merge and are directed to a print position intermediate between the individual positions. At the beginning of a printed segment, it would be necessary to insert six or more guard drops to prevent merging of the first two deflected drops. The loss of six generated drops within a segment was considered too great a reduction in throughput to prevent the slight deterioration in print quality caused by a single merged pair. As noted in the discussion on the merge curves, an increase in separation can enhance the tendency of two drops to merge. For this reason, a guard drop is inserted between the first two deflected drops. The larger ratio of mass/radius of the oversized (merged pair) drop causes it to be decelerated less than a single drop. Thus, the distance between the merged pair and the third deflected drop increases rather than decreases, and a guard drop is not required. Three guard drops are required between the third and fourth deflected drops; two guard drops between the fourth and fifth deflected drops; and one guard drop separating each remaining pair of drops within the segment. This decrease in the number of guard drops is possible because of the lessening of the aerodynamic forces as one proceeds into the segment. For short segments the pattern can be truncated after any deflected drop. If a scan contains more than one printed segment, a number of uncharged drops, usually five or more, must

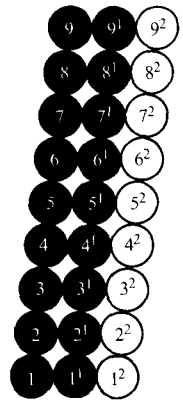

Figure 14 Sequential drop placement.

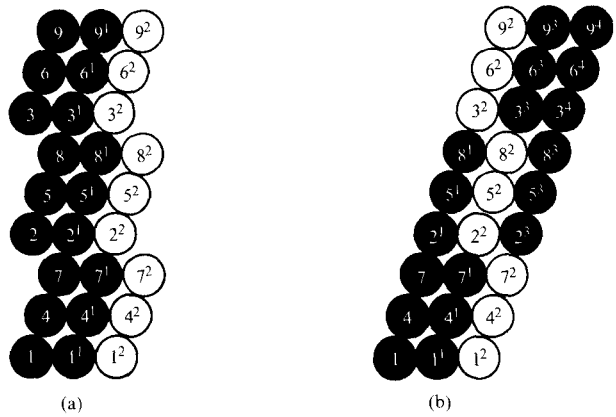

Figure 15 Nonsequential drop placement: (a) single scan and (b) interlace.

Figure 16 "1032" guard drop sequential scheme.

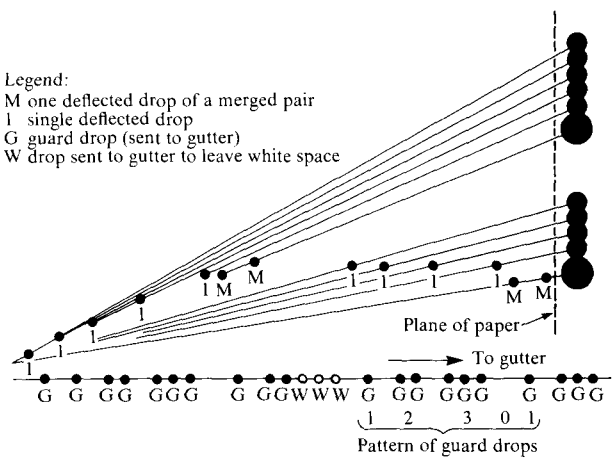

Figure 17 Ink jet print samples with and without drop placement error compensation.

separate the segments to prevent merging of the trailing drop of one segment with the leading drop of the next.

For a given drop generation frequency, the use of a guard drop scheme results in a reduction of throughput. For long segments, the drop utilization efficiency of the "1032" guard drop scheme is $n/(2n+1)$, where n is the number of printed drops.

• *Drop placement error compensation*

The search for a compatible set of operating parameters and drop placement scheme for the ink jet printer involved a number of qualification tests and experiments to verify that printer performance objectives could be achieved. For example, the basic consideration in evaluating the drop placement scheme was to determine whether patterns of drops could be accurately placed at their correct positions in the print plane according to the placement algorithm.

After a satisfactory operating point and placement scheme had been established, it was then necessary to determine experimentally the charge electrode voltages for every allowable pattern of drops in order to compensate for drop placement errors caused by charge induction, electrostatic repulsion, and differential aerodynamic drag. Because of the long-term characteristics of the drop interaction effects, a significant range of drops before and after the reference drop was considered. Drop patterns in our printer included eight leading and three lagging printed drops surrounding the reference drop. For each pattern, charging voltages for the reference drop and surrounding drops were initialized and iteratively adjusted according to an algorithm until all drops were correctly positioned at the paper plane. Data representing the resulting charging voltages are stored in the ink jet printer, and the appropriate voltages are generated from this information each time a particular pattern of drops is printed. In all, nearly 3000 different patterns of drops had to be characterized experimentally to obtain the charging voltages for printing all the allowable drop patterns. An automated system was developed to allow quick and accurate measurement of these experimental data.

An enlarged photograph of compensated and uncompensated ink jet printing is shown in Fig. 17. Drop placement errors due to merging and scattering are evident in the uncompensated printing. Close examination of the defects in the character T reveals some drop placement problems very similar to those illustrated in Figs. 9(a) and (b).

Summary

Development of an ink jet printer capable of producing typewriter print quality required an understanding of the physical effects within the printhead. The phasing of the charge voltage pulse with drop breakoff time had to be controlled to ensure that the proper charge was applied to the drop. Drop charge interactions were found to be significant, both in the charging process, where the intended charge on a drop may be modified, and in the deflection process, where electrostatic repulsion causes drops to scatter. Aerodynamic effects operating on the drops tended to produce drop merging, and a suitable drop placement scheme was developed to prevent merging and allow drops to be accurately placed on their target positions. These combined interaction effects are extremely complex and do not yield readily to theoretical study. Empirical tools and models were developed to aid in understanding their control. A combination of printhead parameters and a print scheme were chosen to allow compensation for the drop misplacement caused by these effects. This compensation had to be made through adjustment of drop charges—the only variable under our control.

Acknowledgments

The authors gratefully acknowledge the contributions of T. H. Williams to the development and evolution of a satisfactory drop placement scheme. Thanks are due also to H. T. Hilton for his work in characterizing the aerodynamic effects in an ink jet system, to H. E. Naylor III for the development of theoretical and experimental models to study the drop charging process, and to W. P. Harbour, Jr., for the design of an automated system to experimentally measure charge electrode voltage drop pattern data. The authors are particularly grateful to M. L. Krieg for his help in the development and use of experimental hardware for drop placement studies and to D. L. Bradley for his support in taking experimental drop placement data.

Appendix 1: Glossary

d_j	jet diameter
v_j	jet velocity
λ	drop-to-drop spacing; wavelength
f	drop frequency
v_d	drop velocity
m_d	drop mass

r_d	drop radius
σ	ink surface tension
ρ	ink density
Q_d	drop charge
V_{ce}	charge electrode voltage
s_{ce}	charge electrode plate spacing
l_{ce}	charge electrode plate length
C_e	equivalent charging capacitance
α	first-order induction factor
β	second-order induction factor
γ	third-order induction factor
ϵ_0	free space permittivity
r_i	drop instability displacement from jet axis
r_0	initial radial displacement of stream from jet axis
z_i	distance from breakup to instability point
t_i	time to instability
x_d	drop deflection
E	electric field
l_{dp}	deflection plate length
z_p	distance from deflection plate entry to print plane

Appendix 2: Charging limit due to drop instability

The electrostatic repulsion force between any two drops of equal charge acting along the stream axis is

$$F = \frac{Q_d^2}{4\pi\epsilon_0\lambda^2}. \tag{A1}$$

Although the electrostatic force is predominantly axial, we assume that a small radial displacement r exists in the stream. This displacement produces a small radial component of the repulsion force, which is proportional to r/λ. The radial acceleration is given by

$$\frac{d^2r}{dt^2} = \frac{1}{m_d}\left(\frac{Q_d^2}{4\pi\epsilon_0\lambda^2}\right)\frac{r}{\lambda}, \tag{A2}$$

where m_d is the drop mass.

Equation (A2) can be solved to yield the time to instability, t_i:

$$t_i = \left[\frac{2Q_d}{4\pi\epsilon_0\lambda^3 m_d}\right]^{\frac{1}{2}} \ln\frac{r_i}{r_0}, \tag{A3}$$

where r_0 is the initial radial displacement of the stream, and r_i is the radial displacement that we define as the criterion for an unstable stream.

The distance from stream breakup to instability is given by

$$z_i = v_j t_i, \tag{A4}$$

and the drop mass is

$$m_d = \frac{\pi d_j^2 \lambda \rho}{4}, \tag{A5}$$

where ρ is ink density. Substituting Eqs. (A4) and (A5) into (A3) and rearranging, we obtain

$$\frac{Q_d z_i}{v_j d_j \lambda^2} = \frac{\pi}{\sqrt{2}}(\rho\epsilon_0)^{\frac{1}{2}} \ln\frac{r_i}{r_0}, \tag{A6}$$

which agrees in form with the empirically obtained Eq. (13).

References

1. W. L. Buehner, J. D. Hill, T. H. Williams, and J. W. Woods, "Application of Ink Jet Technology to a Word Processing Output Printer," *IBM J. Res. Develop.* **21**, 2 (1977, this issue).
2. R. G. Sweet, "High-Frequency Oscillography with Electrostatically Deflected Ink Jets," *Stanford Electronics Laboratories Technical Report No. 1722-1*, Stanford University, CA (March 1964).
3. F. J. Kamphoefner, "Ink Jet Printing," *IEEE Trans. Electron Devices* **ED-19**, 584 (1972).
4. E. Weber, "Method of Electrical Images," *Electromagnetic Theory*, Dover Publications, Inc., New York, 1965.
5. J. W. S. Rayleigh, *Phil. Mag.* **14**, 184 (1882).
6. J. M. Carmichael, "Controlling Print Height in an Ink Jet Printer," *IBM J. Res. Develop.* **21**, 52 (1977, this issue).
7. A. von Engel, *Ionized Gases*, Oxford University Press, London, 1965.
8. H. T. Hilton, private communication.
9. V. E. Bischoff, "Guard Drop Technique for Ink Jet Systems," U.S. Patent 3,562,757 (1971).

Received September 17, 1975; revised August 25, 1976

G. L. Fillmore is located at the IBM Office Products Division laboratory, Boulder, CO 80302; W. L. Buehner and D. L. West are located at the IBM Office Products Division laboratory, Lexington, KY 40507.